

WHY LINEAR SAMPLING REALLY SEEMS TO WORK

MARTIN HANKE

Institute of Mathematics
Johannes Gutenberg-Universität
55099 Mainz, Germany

Dedicated to Gennadi Vainikko on the occasion of his 70th birthday

(Communicated by Lassi Päivärinta)

ABSTRACT. We reconsider the Linear Sampling Method by Colton and Kirsch, and provide an analysis which may serve as a justification of the method for problems where the Factorization Method is known to work. As a by-product, however, we obtain convincing arguments that one popular implementation of the Linear Sampling Method may not be as robust as is commonly believed. Our approach stems from the theory of regularization methods for linear ill-posed operator equations. More precisely, we derive a novel asymptotic analysis of the Tikhonov method if the exact right-hand side is inconsistent, i.e., does not belong to the (dense) range of the corresponding operator. It appears possible that our results can be a starting point to derive a calibration of standard implementations of the Linear Sampling Method, in order to obtain reconstructions of the scattering obstacles that go beyond an approximate localization of their respective positions.

1. Introduction. The *Linear Sampling Method* has been introduced by Colton and Kirsch in their seminal paper [5] to reconstruct one or several unknown acoustic scatterers from the far field information of scattered waves. Its striking features are its simplicity (the nonlinear inverse problem is reduced to a sequence of linear problems with the same operator) and its generality (no a priori information about the scatterer(s) is required: neither their number nor their physical properties need to be known).

The Linear Sampling Method has since been applied successfully to a number of inverse scattering problems, differing in their physical framework or the type of data that are to be used for the reconstruction, cf., e.g., [4, 7, 10, 13, 19]. Today, the method belongs to the state of the art techniques in inverse scattering, as is demonstrated by its treatment in pertinent monographs, e.g., in [3, 6, 15, 16].

Despite its success, however, the Linear Sampling Method still lacks a rigorous justification. Throughout the literature the method is usually motivated in much the same way as in the original source [5], although this motivation cannot bear up against a critical examination, cf. Arens [1], or Section 2 below; another attempt from [1] to explain its success suffers from a similar shortcoming as the original one, cf. Remark 3.2.

2000 *Mathematics Subject Classification.* Primary: 35R30, 65N21.

Key words and phrases. Inverse scattering, sampling method, factorization method.

Arens' paper also established a certain link between the Linear Sampling Method and another method developed by Kirsch [14] shortly after his original paper with Colton, the so-called *Factorization Method*. Unlike the Linear Sampling Method, the Factorization Method has rigorous theoretical grounds in a large variety of important applications; we refer to Kirsch and Grinberg [15] for a detailed exposition of this method. According to [1] an appropriate postprocessing of relevant quantities of the Linear Sampling Method can be used to achieve an equivalent of the Factorization Method (see also Arens and Lechleiter [2] and the account in [15, Section 11]). This observation, however, does not explain the good performance of the *original* Linear Sampling Method, so we shall not delve into this in more detail.

In this paper we provide a qualitative and quantitative analysis of the Linear Sampling Method, and give an interpretation of our results for cases where the Factorization Method is also known to work. To this end we formally restrict our treatment to the specific case of acoustic scattering by sound-soft obstacles. Our analysis, however, extends to other cases of interest, as it only exploits general techniques from the theory of linear ill-posed problems. More precisely, our main tool is a careful investigation of the Tikhonov regularization method and the discrepancy principle for linear operator equations with *inconsistent* right-hand sides and, possibly, perturbed operators.

To begin with, Section 2 gives a very brief introduction to the Linear Sampling Method for the inverse obstacle problem in acoustic scattering. As we will see, the Linear Sampling Method comes with a number of free parameters that can be tuned to optimize the numerical results. We focus on two particular implementations of the method, cf. Section 3, which appear to be most sophisticated. In Sections 4 and 5 we pause to prove the aforementioned auxiliary results about Tikhonov regularization with inconsistent right-hand sides; readers who are mainly interested in the Linear Sampling Method may skip these technical details and jump right away to Section 6 where our findings are used to illuminate the performance of the Linear Sampling Method, which we consider to be the major achievement of this work. In Sections 7 and 8 we conclude with illustrating examples, both numerical and theoretical ones.

2. Problem setting. As our basic setting we consider the inverse obstacle problem in acoustic scattering, where one or several sound-soft acoustic scatterer(s), whose support is denoted by $\Omega \subset \mathbb{R}^2$, are illuminated by time harmonic acoustic waves with wave number $k > 0$. Throughout we assume that Ω is the bounded complement of a domain in \mathbb{R}^2 , that its interior is nonempty and its boundary is sufficiently smooth, and that k^2 is not a Dirichlet eigenvalue of the negative Laplacian in Ω . We restrict ourselves to two space dimensions because this will correspond to our numerical examples. Our analysis, however, can easily be generalized to three space dimensions.

Given a time harmonic incident plane wave

$$u^i(x) = e^{ikd \cdot x}, \quad x \in \mathbb{R}^2,$$

where the direction d belongs to the unit sphere $S \subset \mathbb{R}^2$, scattering obstacles cause a field u which solves the exterior boundary value problem for the Helmholtz equation,

$$(1) \quad \Delta u + k^2 u = 0 \quad \text{in } \mathbb{R}^2 \setminus \Omega, \quad u = -u^i \quad \text{on } \partial\Omega,$$

together with the Sommerfeld radiation condition

$$(2) \quad \frac{\partial u}{\partial r} - iku = o(1/\sqrt{r}), \quad \text{as } r = |x| \rightarrow \infty.$$

Under the given assumptions problem (1), (2) has a unique solution $u \in C^2(\mathbb{R}^2 \setminus \Omega) \cap C(\overline{\mathbb{R}^2 \setminus \Omega})$, and this solution has an asymptotic expansion of the form

$$u(r\hat{x}) = \frac{e^{ikr}}{\sqrt{r}} u_\infty(\hat{x}) + O(r^{-3/2}), \quad \hat{x} \in S, \quad r \rightarrow \infty,$$

cf., e.g., Colton and Kress [6]. The function $u_\infty = u_\infty(\cdot; d) \in \mathcal{L}^2(S)$ is the so-called far field pattern of the scattered wave. This is the measured quantity for our nonlinear inverse problem of interest:

Given the far field $u_\infty(\hat{x}; d)$ for all $\hat{x} \in S$ and all incident directions $d \in S$, determine the support Ω of the scatterer(s).

The given data $u_\infty(\hat{x}; d)$ can be used as integral kernel to define the so-called far field operator

$$(3) \quad Ff(\hat{x}) = \int_S u_\infty(\hat{x}; d)f(d) \, ds(d), \quad \hat{x} \in S,$$

which maps an incident Herglotz wave of the form

$$v(x) = \int_S e^{ikd \cdot x} f(d) \, ds(d), \quad x \in \mathbb{R}^2,$$

onto the far field pattern of the corresponding scattered wave u of (1), (2), where u^i is replaced by v in (1). This operator $F : \mathcal{L}^2(S) \rightarrow \mathcal{L}^2(S)$ is compact, injective, and has dense range, i.e.,

$$(4) \quad \overline{\mathcal{R}(F)} = \mathcal{L}^2(S),$$

cf., e.g., [6, Corollary 3.18].

The focus of the Linear Sampling Method is on the (linear) operator equation

$$(5) \quad Ff = g,$$

where the right-hand side

$$(6) \quad g(\hat{x}) = \frac{e^{i\pi/4}}{\sqrt{8\pi k}} e^{-ik\hat{x} \cdot z}, \quad \hat{x} \in S,$$

is the far field pattern of the fundamental solution of the Helmholtz equation with singularity in the parameter point $z \in \mathbb{R}^2$. Note, however, that equation (5) hardly ever has a solution $f \in \mathcal{L}^2(S)$ (see [5], or Section 7 below). Instead, the true motivation for studying (5) stems from the observation that there are known approximate solutions \bar{f}^δ of (5) satisfying

$$(7) \quad \|F\bar{f}^\delta - g\| \leq \delta$$

for some fixed $\delta > 0$, such that $\|\bar{f}^\delta\|$ goes to infinity as z approaches $\partial\Omega$ from the interior, cf. [5]; here and below, we always denote by $\|\cdot\|$ the norm of $\mathcal{L}^2(S)$. Implementations of the Linear Sampling Method therefore aim to solve the far field equation (5) numerically for various sampling points z within some region of interest where the scatterer(s) are supposed to be, and somehow measure the “failure” of this solution process as a function of z . This is the reason why the method is called “sampling method”.

As pointed out by Arens [1], however, this motivating statement is a triviality from a pure functional analytic point of view, because the far field operator F is compact. Accordingly, equation (5) is always an ill-posed problem, *regardless* what kind of right-hand side is used in (5). This implies that for every parameter point z it is possible to construct approximate solutions with arbitrarily large norm that satisfy (7). Therefore the aforementioned “motivation” provides no information at all about the support of the obstacle(s), and a more profound analysis is required to understand whether and why the Linear Sampling Method really works.

3. Two implementations of the linear sampling method. As the far field equation (5) is ill-posed, all implementations of the Linear Sampling Method involve some sort of regularization to compute approximate solutions, see, for example, Tacchino, Coyle, and Piana [20] for a list and numerical comparison of various options. In view of (7) one of the most straightforward ones is the *Morozov discrepancy principle* [17], i.e., to determine an approximate solution f^δ of (5) from the variational principle

$$(8) \quad f^\delta = \operatorname{argmin} \{ f \in \mathcal{L}^2(S) : \|Ff - g\| \leq \delta \}.$$

In general, f^δ will be different from the particular function \bar{f}^δ mentioned above, but by construction we always have

$$(9) \quad \|\bar{f}^\delta\| \geq \|f^\delta\|.$$

Therefore, if the Morozov approximation has large norm, the same must hold true for the norm of \bar{f}^δ .

It is well-known, cf., e.g., Groetsch [12], that the Morozov principle is connected to Tikhonov’s regularization method, and that the solution f^δ of (8) can be represented as

$$(10) \quad f^\delta = F^*(FF^* + \alpha_\delta I)^{-1}g,$$

where $\alpha_\delta > 0$ is the so-called regularization parameter that is implicitly determined from the nonlinear equation

$$(11) \quad \|Ff^\delta - g\| = \|\alpha_\delta(FF^* + \alpha_\delta I)^{-1}g\| = \delta.$$

In practice, on the other hand, the far field data are contaminated by measurement errors and only known on some discrete subset of $S \times S$. In this case the given data only suffice to compute an approximation \tilde{u}_∞ of u_∞ to be used in (3), in which case the resulting operator \tilde{F} will only be an approximation of F with, say,

$$(12) \quad \|\tilde{F} - F\|_{\mathcal{L}^2(S) \rightarrow \mathcal{L}^2(S)} \leq \|\tilde{u}_\infty - u_\infty\|_{\mathcal{L}^2(S \times S)} =: \varepsilon,$$

where $\|\cdot\|_{\mathcal{L}^2(S) \rightarrow \mathcal{L}^2(S)}$ is the associated operator norm. In this case the triangle inequality yields

$$(13) \quad \|\tilde{F}\bar{f}^\delta - g\| \leq \|(\tilde{F} - F)\bar{f}^\delta\| + \|F\bar{f}^\delta - g\| \leq \varepsilon\|\bar{f}^\delta\| + \delta.$$

Accordingly, one would like to replace δ in (8) by the somewhat larger bound $\varepsilon\|\bar{f}^\delta\| + \delta$, but unfortunately, this bound is not computable as \bar{f}^δ is not available.

The usual remedy is to replace \bar{f}^δ in the upper bound of (13) by an appropriate Tikhonov approximation. More precisely, one computes

$$(10') \quad f^{\delta,\varepsilon} = \tilde{F}^*(\tilde{F}\tilde{F}^* + \alpha_{\delta,\varepsilon}I)^{-1}g,$$

and selects the corresponding regularization parameter $\alpha_{\delta,\varepsilon}$ from the *modified discrepancy principle*

$$(11') \quad \|\tilde{F}f^{\delta,\varepsilon} - g\| = \|\alpha_{\delta,\varepsilon}(\tilde{F}\tilde{F}^* + \alpha_{\delta,\varepsilon}I)^{-1}g\| = \varepsilon\|f^{\delta,\varepsilon}\| + \delta.$$

Although $f^{\delta,\varepsilon}$ cannot be motivated by a variational principle similar to (8), the following proposition shows that (9) still holds when f^δ is replaced by $f^{\delta,\varepsilon}$.

Proposition 3.1. *Assume that $g \neq 0$ and F has dense range. Furthermore, let ε of (12) and δ be two nonnegative parameters, not both of them being zero at the same time. If Problem (10'), (11') is solvable then its solution $f^{\delta,\varepsilon}$ is uniquely determined and satisfies*

$$\|f^{\delta,\varepsilon}\| \leq \|\bar{f}^\delta\|.$$

Moreover, this solution exists whenever δ and ε are sufficiently small.

Proof. The unique solvability of the system (10'), (11') for sufficiently small parameters δ and ε has been verified in [18, Lemma 19]. To prove the second assertion we assume that

$$(14) \quad \|\bar{f}^\delta\| < \|f^{\delta,\varepsilon}\|,$$

so that we have

$$\|\tilde{F}\bar{f}^\delta - g\| \leq \varepsilon\|\bar{f}^\delta\| + \delta < \varepsilon\|f^{\delta,\varepsilon}\| + \delta$$

according to (13). However, by the Morozov principle, $f^{\delta,\varepsilon}$ has minimal norm among all elements $f \in \mathcal{L}^2(S)$ that satisfy

$$\|\tilde{F}f - g\| \leq \varepsilon\|f^{\delta,\varepsilon}\| + \delta,$$

in contradiction to our assumption (14). □

Different implementations of the Linear Sampling Method can differ in the specific regularization method that is used, but also in how they measure the “degree of (un)solvability” of the far field equation (5). Here we consider two possibilities:

- The first one (Method I) is the usual form of the method as described, for example, in the book by Cakoni and Colton [3]. It is based on the norm of the regularized solution $f^{\delta,\varepsilon}$ of (10'), (11'): A large norm is taken to indicate that z is either outside of Ω or close to its boundary.
- The second one (Method II) has been suggested by Colton, Piana, and Potthast [8]. It takes course to the particular value of the regularization parameter $\alpha_{\delta,\varepsilon}$ in (10'), (11'). A small regularization parameter indicates that the far field equation allows only very little regularization to approximate the data within a given accuracy (see also (22) below). Accordingly, the corresponding approximate solution will have a larger norm.

In practice the parameters ε and δ are usually kept fixed, and the resulting numbers $\|f^{\delta,\varepsilon}\|$ and $\alpha_{\delta,\varepsilon}$ are considered to be real valued functions of the parameter $z \in \mathbb{R}^2$. In the end the numerical “reconstructions” of Ω are nothing else than color coded plots of these functions. In our analysis of the Linear Sampling Method we will elaborate on the qualitative form of these plots in the asymptotic regime where one of the two parameters ε and δ is zero and the other one is close to zero. We will also indicate a possibility to obtain quantitative reconstructions of Ω by looking at specific level lines of these functions.

Remark 3.2. We emphasize that every implementation of the Linear Sampling Method needs a specification of the particular regularization method *and* the corresponding rule for the choice of the regularization parameter, because otherwise the norm of the approximate solutions can be made arbitrarily large, or small, by tuning the regularization parameter appropriately, cf., e.g., [12, Corollary 2.1.3]. It is for this reason that Corollary 3.4 in [1] is of no use, either, to explain the performance of the Linear Sampling Method.

4. Auxiliary results about the discrepancy principle: The case $\varepsilon = 0$. For the time being let us investigate the equation

$$(15) \quad Ff = g$$

with a general right-hand side $g \in \mathcal{L}^2(S)$ and F as above. We mention, however, that all the results in this and the following section hold for general operators F between two Hilbert spaces X and Y ; all that we require is that the range $\mathcal{R}(F)$ of F is dense in Y .

The (modified) discrepancy principle has been analyzed in detail by Vainikko [21, 22] under the assumption that (15) has a solution $f \in \mathcal{L}^2(S)$. His analysis exhibits a crucial role of so-called source conditions for either the solution or, equivalently, the right-hand side of (15). We define the nested linear spaces

$$(16) \quad \mathcal{R}(|F|^\nu) = \mathcal{R}((FF^*)^{\nu/2}), \quad \nu \geq 0,$$

cf., e.g., [9, Section 3.2], which satisfy the property

$$(17) \quad \mathcal{R}(|F|^\nu) \subsetneq \mathcal{R}(|F|^\mu) \quad \text{when } 0 \leq \mu < \nu.$$

Note that

$$(18) \quad \mathcal{R}(|F|^0) = \mathcal{L}^2(S) \quad \text{and} \quad \mathcal{R}(|F|^1) = \mathcal{R}(F).$$

It is said that g satisfies the *source condition* $g \in \mathcal{R}(|F|^\nu)$ for some $\nu > 0$, if and only if there is some $w \in \mathcal{L}^2(S)$ such that

$$(19) \quad g = (FF^*)^{\nu/2}w.$$

In particular, cf. (18), equation (15) has a solution $f \in \mathcal{L}^2(S)$, if and only if g satisfies the source condition (19) for some $\nu \geq 1$.

Consider now the Tikhonov approximation

$$(20) \quad f_\alpha = \tilde{F}^*(\tilde{F}\tilde{F}^* + \alpha I)^{-1}g$$

where

$$\|\tilde{F} - F\| \leq \varepsilon,$$

and the regularization parameter $\alpha > 0$ is determined from the modified discrepancy principle

$$(21) \quad \|\tilde{F}f_\alpha - g\| = \tau(\varepsilon\|f_\alpha\| + \delta),$$

where $\tau \geq 1$ is some fixed parameter. If $\tau > 1$ then one of Vainikko's results from [21] states that the regularization parameter α satisfies

$$(22) \quad \alpha \geq c(\varepsilon + \delta)^{2/\nu},$$

provided that g satisfies the source condition (19) for some $\nu \in [1, 2]$ and that ε and δ are sufficiently small; in (22) and throughout this paper the constant c denotes a generic positive constant, independent of ε and δ , but depending on the particular function g via the source w from (19). The inequality (22) may be interpreted as

follows: With increasing regularity of the right-hand side, i.e., with increasing ν , more regularization is admissible without violating the discrepancy principle. Or, to put it the other way round, when the problem is getting hard, i.e., when ν gets small, only little regularization is tolerable to determine a viable approximate solution.

Vainikko’s analysis is restricted to source conditions (19) with exponents $\nu \geq 1$, and thus is not applicable in our context. However, his result and many more from the general theory of linear ill-posed problems (cf., e.g., [9]) suggest to relax this constraint and to study exponents $0 < \nu \leq 1$ to analyze the present situation. One of the outcomes of our analysis is that for $\nu \in (0, 1)$ the two parameters ε and δ in (21) have a different impact, in contrast to their role in (22), say. To simplify our analysis we will study these parameters separately by setting the other one to zero in either case.

We start with the classical instance where F is given exactly, i.e., when $\varepsilon = 0$. The case $\varepsilon > 0$ will be postponed to Section 5. Concerning the case $\varepsilon = 0$ we first quote from [12, Theorem 3.3.1] or [18, Section 7] that problem (20), (21) is uniquely solvable whenever $0 < \delta < \|g\|/\tau$. Moreover, for fixed $\tau \geq 1$ the corresponding regularization parameter $\alpha = \alpha(\delta)$ is a continuous and strictly monotonically increasing function of δ with

$$\lim_{\delta \rightarrow 0} \alpha(\delta) = 0 \quad \text{and} \quad \lim_{\delta \rightarrow \|g\|/\tau} \alpha(\delta) = \infty.$$

Without loss of generality we restrict our attention to the fixed parameter $\tau = 1$ in the sequel.

Theorem 4.1. *Let g satisfy the source condition (19) for some $w \in \mathcal{L}^2(S)$ and $0 < \nu \leq 1$, and, for $0 < \delta < \|g\|$ let f_α of (20) with $\tilde{F} = F$ and corresponding regularization parameter α be defined by*

$$(23) \quad \|Ff_\alpha - g\| = \delta.$$

Then we have

$$(24) \quad \|f_\alpha\| \leq c\delta^{\frac{\nu-1}{\nu}}$$

and

$$(25) \quad \alpha \geq c\delta^{2/\nu}.$$

For $0 < \nu < 1$ the somewhat stronger asymptotics

$$(26) \quad \|f_\alpha\| = o(\delta^{\frac{\nu-1}{\nu}}) \quad \text{and} \quad \alpha^\nu/\delta^2 \rightarrow \infty$$

hold as δ goes to zero.

Proof. Rewriting $g = (FF^*)^{\nu/2}w$ we conclude from (20) that

$$\begin{aligned} \|f_\alpha\| &= \|(FF^*)^{1/2}(FF^* + \alpha I)^{-1}g\| \\ &= \|(FF^*)^{(\nu+1)/2}(FF^* + \alpha I)^{-1}w\| \\ &\leq \|(FF^*)^{(\nu+1)/2}(FF^* + \alpha I)^{-1}\| \|w\|. \end{aligned}$$

The operator norm can be estimated using spectral theoretical arguments, namely

$$\begin{aligned} \|(FF^*)^{(\nu+1)/2}(FF^* + \alpha I)^{-1}\| &\leq \sup_{\lambda > 0} \frac{\lambda^{(\nu+1)/2}}{\lambda + \alpha} \\ &= \frac{1}{2} (1 + \nu)^{(1+\nu)/2} (1 - \nu)^{(1-\nu)/2} \alpha^{(\nu-1)/2}, \end{aligned}$$

and hence, we have

$$(27) \quad \|f_\alpha\| \leq c\alpha^{(\nu-1)/2}.$$

Note that $\nu \leq 1$, and hence the desired estimate (24) follows readily from (25), once the latter has been verified.

To this end we remark that, similar to above, we have

$$\|(FF^*)^{\nu/2}(FF^* + \alpha I)^{-1}\| \leq \sup_{\lambda > 0} \frac{\lambda^{\nu/2}}{\lambda + \alpha} = \frac{1}{2} \nu^{\nu/2} (2 - \nu)^{1-\nu/2} \alpha^{\nu/2-1},$$

and hence,

$$(28) \quad \|Ff_\alpha - g\| = \alpha \|(FF^*)^{\nu/2}(FF^* + \alpha I)^{-1}w\| \leq c\alpha^{\nu/2}.$$

It therefore follows from (11) that

$$\delta = \|Ff_\alpha - g\| \leq c\alpha^{\nu/2}.$$

and thus we have established (25).

To prove the remaining assertions (26) we need to refine the previous estimate. Since $\alpha = \alpha(\delta)$ is an increasing continuous function of δ with $\alpha \rightarrow 0$ as $\delta \rightarrow 0$, we can choose $\gamma = \gamma(\delta)$ such that

$$(29) \quad \alpha = o(\gamma) \quad \text{and} \quad \gamma = o(1) \quad \text{as} \quad \delta \rightarrow 0;$$

for example, we can pick $\gamma(\delta) = \sqrt{\alpha(\delta)}$. Next we note that the function

$$\lambda \mapsto \frac{\lambda^{\nu/2}}{\lambda + \alpha}$$

is monotonically decreasing for $\lambda > \lambda_* = \nu\alpha/(2 - \nu)$. As a consequence, we have

$$(30) \quad \sup_{\lambda > \gamma} \frac{\lambda^{\nu/2}}{\lambda + \alpha} = \frac{\gamma^{\nu/2}}{\gamma + \alpha} \leq \gamma^{\nu/2-1}$$

for δ sufficiently small. Now we need to introduce the spectral family $\{E_\lambda\}_\lambda$ of the operator FF^* , cf., e.g., [9, Section 2.3]. Then we can rewrite $w = E_\gamma w + (I - E_\gamma)w$ and obtain

$$\begin{aligned} \delta &\leq \alpha \|(FF^*)^{\nu/2}(FF^* + \alpha I)^{-1}E_\gamma w\| \\ &\quad + \alpha \|(FF^*)^{\nu/2}(FF^* + \alpha I)^{-1}(I - E_\gamma)w\| \\ &\leq \alpha \|(FF^*)^{\nu/2}(FF^* + \alpha I)^{-1}\| \|E_\gamma w\| \\ &\quad + \alpha \|(FF^*)^{\nu/2}(FF^* + \alpha I)^{-1}(I - E_\gamma)\| \|w\| \\ &\leq c\alpha^{\nu/2} (\|E_\gamma w\| + (\alpha/\gamma)^{1-\nu/2} \|w\|). \end{aligned}$$

According to (29) the expression in paranthesis goes to zero as $\delta \rightarrow 0$, and hence,

$$\alpha^\nu / \delta^2 \rightarrow \infty \quad \text{as} \quad \delta \rightarrow 0,$$

as was to be shown. For $0 < \nu < 1$ this implies that

$$\alpha^{(\nu-1)/2} \delta^{\frac{1-\nu}{\nu}} \rightarrow 0 \quad \text{as} \quad \delta \rightarrow 0,$$

and inserting this into (27) the first asymptotics in (26) follows as well. \square

We mention in passing that estimate (25) of Theorem 4.1 matches Vainikko's estimates (22) when $\varepsilon = 0$. The focus of our interest, however, is on the case $0 < \nu \leq 1$. In this case the upper bound (24) for $\|f_\alpha\|$ goes to infinity as $\delta \rightarrow 0$ when $0 < \nu < 1$; it remains finite for the extreme case $\nu = 1$, i.e., when $g \in \mathcal{R}(F)$,

where f_α converges to a solution of (15) as $\delta \rightarrow 0$, and hence, estimate (24) is sharp for $\nu = 1$.

On the other hand, both estimates (24) and (25) fail to be real sharp for $0 < \nu < 1$, as is demonstrated in (26). In the remainder of this section we will investigate this issue somewhat further and prove two converse results which show that the exponents in (24), (25), are best possible.

Theorem 4.2. *Assume that for some given $g \in \mathcal{L}^2(S)$ the regularization parameter α of (23) satisfies $\alpha \geq c\delta^{2/\nu}$ for some $0 < \nu \leq 2$ and all $\delta > 0$ sufficiently small. Then $g \in \mathcal{R}(|F|^\mu)$ for every $0 \leq \mu < \nu$. If $\nu = 2$ then we have $g \in \mathcal{R}(FF^*)$.*

Proof. For ease of notation we introduce the nondecreasing lower semicontinuous function

$$(31) \quad \eta(\lambda) = \langle E_\lambda g, g \rangle = \|E_\lambda g\|^2, \quad \lambda \in \mathbb{R}.$$

(Note that for compact operators F like the far field operator (3) η is a piecewise constant step function.) Then we can rewrite (11) and estimate

$$(32) \quad \begin{aligned} \delta^2 &= \int_0^\infty \left(\frac{\alpha}{\lambda + \alpha}\right)^2 d\eta(\lambda) \geq \int_0^\alpha \left(\frac{\alpha}{\lambda + \alpha}\right)^2 d\eta(\lambda) \geq \frac{1}{4} \int_0^\alpha d\eta(\lambda) \\ &= \frac{1}{4} \|E_\alpha g\|^2. \end{aligned}$$

Together with the assumption (25) we thus have

$$\|E_\alpha g\| = O(\alpha^{\nu/2}),$$

the constant in the $O(\cdot)$ notation being independent of the particular value of δ . Now, as δ runs through some interval $(0, \delta_*]$, $\alpha = \alpha(\delta)$ attains all values within some interval $(0, \alpha_*]$. Therefore the first assertion of Theorem 4.2 follows from [9, Lemma 4.12].

If $\nu = 2$, i.e., $\alpha \geq c\delta$, then we conclude from (11) that

$$\delta = \|\alpha(FF^* + \alpha I)^{-1}g\| \geq c\delta \|(FF^* + \alpha I)^{-1}g\|,$$

i.e., $w_\alpha = (FF^* + \alpha I)^{-1}g$ remains bounded as α goes to zero. Accordingly, there is a sequence $(\alpha_n)_n$ with $\alpha_n \rightarrow 0$ as $n \rightarrow \infty$ such that w_{α_n} converges weakly to some $w \in \mathcal{L}^2(S)$. It follows that $FF^*w_{\alpha_n} \rightharpoonup FF^*w$, and hence,

$$g = (FF^* + \alpha_n I)w_{\alpha_n} = FF^*w_{\alpha_n} + \alpha_n w_{\alpha_n} \rightharpoonup FF^*w.$$

Accordingly, $g \in \mathcal{R}(FF^*)$, as was to be shown. □

Concerning the rate of divergence of $\|f_\alpha\|$ we can establish a similar result.

Theorem 4.3. *Assume that for some fixed $g \in \mathcal{L}^2(S)$ the solution f_α of (23) satisfies $\|f_\alpha\| \leq c\delta^{(\nu-1)/\nu}$ for some $0 < \nu \leq 1$ and all $\delta > 0$ sufficiently small. Then $g \in \mathcal{R}(|F|^\mu)$ for every $0 \leq \mu < \nu$. If $\nu = 1$ then we have $g \in \mathcal{R}(F)$.*

Proof. We use the same notation as in Theorem 4.2. Let $\alpha_j = 2^{-j}\alpha_*$, $j = 0, 1, 2, \dots$, and denote by δ_j the associated value of the regularization parameter for which

$\alpha(\delta_j) = \alpha_j$. Then, for $0 < \mu < \nu$ we have

$$\begin{aligned} \int_{\alpha_{n-}}^{\alpha_*} \lambda^{-\mu} d\eta(\lambda) &= \sum_{j=1}^n \int_{\alpha_{j-}}^{2\alpha_j} \lambda^{-\mu} d\eta(\lambda) = \sum_{j=1}^n \int_{\alpha_{j-}}^{2\alpha_j} \lambda^{\nu-\mu} \lambda^{-\nu} d\eta(\lambda) \\ &\leq \sum_{j=1}^n (2\alpha_j)^{\nu-\mu} \int_{\alpha_{j-}}^{2\alpha_j} \lambda^{-\nu} d\eta(\lambda) \\ &= \alpha_*^{\nu-\mu} \sum_{j=1}^n (2^{\mu-\nu})^{j-1} \int_{\alpha_{j-}}^{2\alpha_j} \lambda^{-\nu} d\eta(\lambda). \end{aligned}$$

Using Hölder's inequality we can estimate the integral on the last line to obtain

$$\begin{aligned} \int_{\alpha_{j-}}^{2\alpha_j} \lambda^{-\nu} d\eta(\lambda) &\leq \left(\int_{\alpha_{j-}}^{2\alpha_j} \lambda^{-1} d\eta(\lambda) \right)^{\nu} \left(\int_{\alpha_{j-}}^{2\alpha_j} d\eta(\lambda) \right)^{1-\nu} \\ &\leq \left(4 \int_{\alpha_{j-}}^{2\alpha_j} \frac{\lambda}{(\lambda + \alpha_j)^2} d\eta(\lambda) \right)^{\nu} \left(9 \int_{\alpha_{j-}}^{2\alpha_j} \left(\frac{\alpha_j}{\lambda + \alpha_j} \right)^2 d\eta(\lambda) \right)^{1-\nu} \\ &\leq \left(4 \int_0^{\infty} \frac{\lambda}{(\lambda + \alpha_j)^2} d\eta(\lambda) \right)^{\nu} \left(9 \int_0^{\infty} \left(\frac{\alpha_j}{\lambda + \alpha_j} \right)^2 d\eta(\lambda) \right)^{1-\nu} \\ &\leq 9 \|f_{\alpha_j}\|^{2\nu} \|Ff_{\alpha_j} - g\|^{2(1-\nu)}. \end{aligned}$$

By assumption, $\|f_{\alpha_j}\|^{2\nu} \leq c^{2\nu} \delta_j^{2(\nu-1)}$, and hence, using (23), we conclude that

$$\int_{\alpha_{j-}}^{2\alpha_j} \lambda^{-\nu} d\eta(\lambda) \leq 9c^{2\nu} \quad \text{for every } j = 0, 1, 2, \dots$$

Inserting this above we finally obtain that

$$\int_{\alpha_{n-}}^{\alpha_*} \lambda^{-\mu} d\eta(\lambda) \leq 9c^{2\nu} \alpha_*^{\nu-\mu} \sum_{j=0}^{n-1} (2^{\mu-\nu})^j \leq \frac{9c^{2\nu} \alpha_*^{\nu-\mu}}{1 - 2^{\mu-\nu}} < \infty$$

for every $n = 1, 2, \dots$, and hence, that $g \in \mathcal{R}(|F|^\mu)$.

If the assumptions of Theorem 4.3 are valid for $\nu = 1$ then $\|f_\alpha\|$ remains bounded as $\delta \rightarrow 0$. In this case the assertion follows from [9, Proposition 3.6]. \square

We have thus established a strong link between the value of the parameter ν in the source condition (19), and the decay of the regularization parameter α of the discrepancy principle and also the rate of divergence of the corresponding Tikhonov approximations, at least when $\varepsilon = 0$ in (21) and (12).

5. Auxiliary results about the discrepancy principle: The case $\delta = 0$.

A crucial difference between Vainikko's analysis of the discrepancy principle and the present setting within the context of the Linear Sampling Method is in the role of the two parameters ε and δ in (21). While the two parameters have equal weight in the solvable case of [21], they experience a different weighting on the right-hand side of (21) for unsolvable linear equations, as the Tikhonov approximation f_α will blow up in norm as ε and δ go to zero. This has some subtle implications for the analysis of the Linear Sampling Method below. To make this analysis more transparent, and since this is the way the Linear Sampling Method has mostly been implemented in

the literature anyway, we set $\delta = 0$ in the sequel, and focus solely on the role of ε . In other words, we consider

$$(33) \quad f_\alpha = \tilde{F}^*(\tilde{F}\tilde{F}^* + \alpha I)^{-1}g,$$

where the regularization parameter α is given by the nonlinear equation

$$(34) \quad \|\tilde{F}f_\alpha - g\| = \varepsilon\|f_\alpha\|,$$

and \tilde{F} satisfies

$$\|\tilde{F} - F\| \leq \varepsilon.$$

By virtue of Proposition 3.1, problem (33), (34) has a unique solution for $g \neq 0$ and ε sufficiently small. By slight abuse of notation we write $\alpha = \alpha(\varepsilon)$ for the corresponding regularization parameter. For later use we establish a somewhat stronger result than Proposition 3.1 for the case where $\tilde{F} = F$ for every $\varepsilon > 0$.

Proposition 5.1. *Assume that $g \neq 0$, $\tilde{F} = F$ for every $\varepsilon > 0$, and that F has dense range. Then the regularization parameter $\alpha = \alpha(\varepsilon)$ of (33), (34), is a continuous and strictly monotonically increasing function of ε with*

$$\lim_{\varepsilon \rightarrow 0} \alpha(\varepsilon) = 0 \quad \text{and} \quad \lim_{\varepsilon \rightarrow \infty} \alpha(\varepsilon) = \infty.$$

Proof. By virtue of (34) we can consider

$$(35) \quad \varepsilon = \frac{\|Ff_\alpha - g\|}{\|f_\alpha\|}$$

as a function of $\alpha \in (0, \infty)$. The numerator is a strictly increasing continuous function of α while the denominator is continuous and strictly decreasing. As a consequence, $\varepsilon = \varepsilon(\alpha)$ is a continuous and strictly increasing function. In the limit, when $\alpha \rightarrow 0$ the numerator of (35) converges to zero while the denominator either goes to infinity, or stays away from zero. Hence, ε can be extended continuously by zero for $\alpha = 0$. As $\alpha \rightarrow \infty$ the numerator converges to $\|g\|$ whereas the denominator converges to zero. Accordingly, $\varepsilon \rightarrow \infty$ as $\alpha \rightarrow \infty$. Thus, $\varepsilon = \varepsilon(\alpha)$ is a strictly monotonic and continuous mapping of $[0, \infty)$ onto itself which has a strictly monotonic continuous inverse mapping $\alpha = \alpha(\varepsilon)$, which has all the required properties. \square

We now consider the maximal rate of divergence of the regularized solutions as $\varepsilon \rightarrow 0$.

Theorem 5.2. *Let g satisfy (19) for some $w \in \mathcal{L}^2(S) \setminus \{0\}$ and $0 < \nu < 1$, and let f_α be the solution of (33), (34), where $\|\tilde{F} - F\| \leq \varepsilon$. Then we have*

$$(36) \quad \|f_\alpha\| \leq c\varepsilon^{\nu-1}.$$

Proof. We need to distinguish two cases. In the first case we assume that

$$(37) \quad \alpha \geq \frac{1-\nu}{1+\nu}\varepsilon^2,$$

and refer to (27) and (28) to estimate

$$\begin{aligned}
\|f_\alpha\| &= \|\tilde{F}^*(\tilde{F}\tilde{F}^* + \alpha I)^{-1}g\| \\
&\leq \|F^*(FF^* + \alpha I)^{-1}g\| + \|(\tilde{F}^* - F^*)(FF^* + \alpha I)^{-1}g\| \\
&\quad + \|\tilde{F}^*((\tilde{F}\tilde{F}^* + \alpha I)^{-1} - (FF^* + \alpha I)^{-1})g\| \\
&\leq c\alpha^{(\nu-1)/2} + \|\tilde{F}^* - F^*\| \|(FF^* + \alpha I)^{-1}g\| \\
&\quad + \|\tilde{F}^*((\tilde{F}\tilde{F}^* + \alpha I)^{-1} - (FF^* + \alpha I)^{-1})g\| \\
&\leq c\alpha^{(\nu-1)/2} + c\varepsilon\alpha^{(\nu-2)/2} + \|\tilde{F}^*((\tilde{F}\tilde{F}^* + \alpha I)^{-1} - (FF^* + \alpha I)^{-1})g\|.
\end{aligned}$$

Following [21] we rewrite the operator in parenthesis in the final term as

$$\begin{aligned}
&(\tilde{F}\tilde{F}^* + \alpha I)^{-1} - (FF^* + \alpha I)^{-1} \\
(38) \quad &= (\tilde{F}\tilde{F}^* + \alpha I)^{-1}(F - \tilde{F})F^*(FF^* + \alpha I)^{-1} \\
&\quad + (\tilde{F}\tilde{F}^* + \alpha I)^{-1}\tilde{F}(F^* - \tilde{F}^*)(FF^* + \alpha I)^{-1},
\end{aligned}$$

and obtain, using (27) and (28) again, that

$$\begin{aligned}
&\|\tilde{F}^*((\tilde{F}\tilde{F}^* + \alpha I)^{-1} - (FF^* + \alpha I)^{-1})g\| \\
&\leq \|\tilde{F}^*(\tilde{F}\tilde{F}^* + \alpha I)^{-1}\| \|F - \tilde{F}\| \|F^*(FF^* + \alpha I)^{-1}g\| \\
&\quad + \|\tilde{F}^*(\tilde{F}\tilde{F}^* + \alpha I)^{-1}\tilde{F}\| \|F^* - \tilde{F}^*\| \|(FF^* + \alpha I)^{-1}g\| \\
&\leq c\alpha^{-1/2}\varepsilon\alpha^{(\nu-1)/2} + c\varepsilon\alpha^{(\nu-2)/2} \\
&= c\varepsilon\alpha^{(\nu-2)/2}.
\end{aligned}$$

Inserting this above, we have thus shown that

$$\|f_\alpha\| \leq c\alpha^{(\nu-1)/2} + c\varepsilon\alpha^{(\nu-2)/2},$$

and since the two exponents of α are negative we can use (37) to achieve the desired bound (36).

In the second case we need to consider the situation where

$$(39) \quad \alpha \leq \frac{1-\nu}{1+\nu} \varepsilon^2.$$

In this case we take into account that the regularization parameter satisfies (34), and hence we have

$$\begin{aligned}
\varepsilon\|f_\alpha\| &= \|\alpha(\tilde{F}\tilde{F}^* + \alpha I)^{-1}g\| \\
(40) \quad &\leq \|\alpha(FF^* + \alpha I)^{-1}g\| + \alpha\|((\tilde{F}\tilde{F}^* + \alpha I)^{-1} - (FF^* + \alpha I)^{-1})g\| \\
&\leq c\alpha^{\nu/2} + \alpha\|((\tilde{F}\tilde{F}^* + \alpha I)^{-1} - (FF^* + \alpha I)^{-1})g\|
\end{aligned}$$

by virtue of (28). To proceed we make another use of the spectral family $\{E_\lambda\}_\lambda$ of FF^* , and rewrite the expression within the norm of the second term as

$$\begin{aligned}
&((\tilde{F}\tilde{F}^* + \alpha I)^{-1} - (FF^* + \alpha I)^{-1})g \\
(41a) \quad &= ((\tilde{F}\tilde{F}^* + \alpha I)^{-1} - (FF^* + \alpha I)^{-1})E_{\varepsilon^2}g \\
(41b) \quad &\quad + (\tilde{F}\tilde{F}^* + \alpha I)^{-1}\tilde{F}(F^* - \tilde{F}^*)(FF^* + \alpha I)^{-1}(I - E_{\varepsilon^2})g \\
(41c) \quad &\quad + (\tilde{F}\tilde{F}^* + \alpha I)^{-1}(F - \tilde{F})F^*(FF^* + \alpha I)^{-1}(I - E_{\varepsilon^2})g,
\end{aligned}$$

cf. (38), and estimate the three terms on the right-hand side separately. For the first term we have

$$\begin{aligned} & \|((\tilde{F}\tilde{F}^* + \alpha I)^{-1} - (FF^* + \alpha I)^{-1})E_{\varepsilon^2}g\| \\ & \leq \left(\|(\tilde{F}\tilde{F}^* + \alpha I)^{-1}\| + \|(FF^* + \alpha I)^{-1}\| \right) \|E_{\varepsilon^2}(FF^*)^{\nu/2}w\|, \end{aligned}$$

and hence,

$$(42a) \quad \|((\tilde{F}\tilde{F}^* + \alpha I)^{-1} - (FF^* + \alpha I)^{-1})E_{\varepsilon^2}g\| \leq \frac{2}{\alpha} \varepsilon^\nu \|w\|.$$

For the second and the third term we first note that, since $\nu < 1$, the two functions

$$\lambda \mapsto \frac{\lambda^{\nu/2}}{\lambda + \alpha} \quad \text{and} \quad \lambda \mapsto \frac{\lambda^{(\nu+1)/2}}{\lambda + \alpha}$$

are strictly decreasing for $\lambda \geq \frac{1+\nu}{1-\nu} \alpha$, and in particular for $\lambda \geq \varepsilon^2$ by virtue of (39). Therefore we can conclude that

$$\begin{aligned} & \|(\tilde{F}\tilde{F}^* + \alpha I)^{-1}\tilde{F}(F^* - \tilde{F}^*)(FF^* + \alpha I)^{-1}(I - E_{\varepsilon^2})g\| \\ (42b) \quad & \leq \|(\tilde{F}\tilde{F}^* + \alpha I)^{-1}\tilde{F}\| \|F^* - \tilde{F}^*\| \|(FF^* + \alpha I)^{-1}(FF^*)^{\nu/2}(I - E_{\varepsilon^2})w\| \\ & \leq \frac{1}{\sqrt{\alpha}} \varepsilon \frac{\varepsilon^\nu}{\varepsilon^2 + \alpha} \|w\| \leq \frac{\varepsilon^{\nu-1}}{\sqrt{\alpha}} \|w\|. \end{aligned}$$

Similarly we obtain that

$$\begin{aligned} & \|(\tilde{F}\tilde{F}^* + \alpha I)^{-1}(F - \tilde{F})F^*(FF^* + \alpha I)^{-1}(I - E_{\varepsilon^2})g\| \\ (42c) \quad & \leq \|(\tilde{F}\tilde{F}^* + \alpha I)^{-1}\| \|F - \tilde{F}\| \|(FF^* + \alpha I)^{-1}(FF^*)^{(\nu+1)/2}(I - E_{\varepsilon^2})w\| \\ & \leq \frac{1}{\alpha} \varepsilon \frac{\varepsilon^{\nu+1}}{\varepsilon^2 + \alpha} \|w\| \leq \frac{\varepsilon^\nu}{\alpha} \|w\|. \end{aligned}$$

Inserting (42) into (41) we thus conclude that

$$\|((\tilde{F}\tilde{F}^* + \alpha I)^{-1} - (FF^* + \alpha I)^{-1})g\| \leq c \left(\frac{\varepsilon^{\nu-1}}{\sqrt{\alpha}} + \frac{\varepsilon^\nu}{\alpha} \right),$$

and, combining this with (40) and (39), we have finally shown that

$$\varepsilon \|f_\alpha\| \leq c (\alpha^{\nu/2} + \varepsilon^{\nu-1}\sqrt{\alpha} + \varepsilon^\nu) \leq c\varepsilon^\nu.$$

This proves assertion (36) also in the second case. □

A few remarks are in order. First, we mention that as in Theorem 4.1 one can refine the above arguments to improve the result of Theorem 5.2 to

$$\|f_\alpha\| = o(\varepsilon^{\nu-1}),$$

whenever g belongs to $\mathcal{R}((FF^*)^{\nu/2})$ with $0 < \nu < 1$. Second, the estimate (36) extends to the case $\nu = 1$, since then we have $g \in \mathcal{R}(F)$, and hence, f_α converges to a solution of (15) as $\varepsilon \rightarrow 0$, cf. [22, Theorem 4]. Third, in contrast to Theorem 4.1, we have not been able to obtain a lower bound for the regularization parameter α of the modified discrepancy principle when $\delta = 0$ and $0 < \nu < 1$. Nonetheless we will exemplify below that, as a rule of thumb, the regularization parameter roughly decays like ε^2 as $\varepsilon \rightarrow 0$, quite independently of the value of ν .

But before we address this problem, we first want to investigate the sharpness of Theorem 5.2. To this end we consider the special case where $\tilde{F} = F$ for every value of $\varepsilon > 0$.

Proposition 5.3. *Let $g \neq 0$ be fixed and f_α be defined by (33), (34), where $\tilde{F} = F$. If $\|f_\alpha\| \leq c\varepsilon^{\nu-1}$ for some $0 < \nu \leq 1$ and all $\varepsilon > 0$, then $g \in \mathcal{R}(|F|^\mu)$ for every $0 \leq \mu < \nu$. If $\nu = 1$ then we have $g \in \mathcal{R}(F)$.*

Proof. We let

$$\delta = \|Ff_\alpha - g\|,$$

and obtain from (34) and the given assumptions that

$$(43) \quad \delta = \varepsilon \|f_\alpha\| \leq c\varepsilon^\nu.$$

Accordingly, f_α is the solution of the classical Morozov discrepancy principle (23) where $\delta \rightarrow 0$ as $\varepsilon \rightarrow 0$. Solving (43) for ε , we obtain $\varepsilon \geq c\delta^{1/\nu}$, and hence, we conclude that

$$\|f_\alpha\| \leq c\varepsilon^{\nu-1} \leq c\delta^{(\nu-1)/\nu}.$$

As δ depends continuously on ε via f_α , cf. Proposition 5.1, we can now apply Theorem 4.3 to obtain the desired result. \square

It follows from this result that the exponent in (36) is best possible under the general assumptions made in Theorem 5.2.

We conclude this section with an example for which we can actually verify that the regularization parameter α decays like ε^2 as $\varepsilon \rightarrow 0$, regardless of the size of the exponent $\nu \in (0, 1)$ in the source condition (19).

Example 1. Let $F : \mathcal{L}^2(0, 1) \rightarrow \mathcal{L}^2(0, 1)$ be such that FF^* is the multiplication operator

$$(44) \quad (FF^*g)(t) = tg(t), \quad g \in \mathcal{L}^2(0, 1), \quad t \in (0, 1).$$

Then the spectral measure η of (31) is given by

$$\eta(\lambda) = \langle E_\lambda g, g \rangle = \int_0^\lambda |g(t)|^2 dt, \quad t \in (0, 1),$$

and the function

$$(45) \quad g(t) = t^{(\nu-1)/2}, \quad t \in (0, 1),$$

belongs to $\mathcal{R}(|F|^\mu)$ whenever $0 < \mu < \nu < 1$.

For this particular g of (45) and for $\tilde{F} = F$ we compute

$$\begin{aligned} \alpha \|f_\alpha\|^2 &= \int_0^1 \frac{\alpha\lambda}{(\alpha + \lambda)^2} d\eta(\lambda) = \frac{1}{\alpha} \int_0^1 \frac{\lambda^\nu}{(1 - \beta\lambda)^2} d\lambda \\ &= \frac{1}{\alpha} \frac{1}{\nu + 1} F(2, \nu + 1; \nu + 2; \beta), \end{aligned}$$

where $\beta = -1/\alpha$ and F is the hypergeometric function. From the asymptotic behavior of the hypergeometric function, cf., e.g., Gradshteyn and Ryzhik [11, 9.132], thus follows that

$$\alpha \|f_\alpha\|^2 \sim \nu \frac{\pi}{\sin(\nu\pi)} \alpha^\nu, \quad \alpha \rightarrow 0.$$

In a similar fashion we obtain that

$$\begin{aligned} \|Ff_\alpha - g\|^2 &= \int_0^1 \frac{\alpha^2}{(\alpha + \lambda)^2} d\eta(\lambda) = \int_0^1 \frac{\lambda^{\nu-1}}{(1 - \beta\lambda)^2} d\lambda \\ &= \frac{1}{\nu} F(2, \nu; \nu + 1; \beta) \sim (1 - \nu) \frac{\pi}{\sin(\nu\pi)} \alpha^\nu, \end{aligned}$$

and we therefore conclude from (34) that

$$\varepsilon^2 = \alpha \frac{\|Ff_\alpha - g\|^2}{\alpha\|f_\alpha\|^2} \sim \frac{1 - \nu}{\nu} \alpha, \quad \alpha \rightarrow 0,$$

i.e., that

$$(46) \quad \alpha \sim \frac{\nu}{1 - \nu} \varepsilon^2, \quad \varepsilon \rightarrow 0,$$

for g of (45) and $\tilde{F} = F$ for every $\varepsilon > 0$. □

Unfortunately, concerning our analysis of the Linear Sampling Method, this example is only of limited value, because the far field operator, unlike the multiplication operator (44), is a compact operator with a discrete spectrum. We expect that for compact operators the decay of $\alpha = \alpha(\varepsilon)$ is more irregular as $\varepsilon \rightarrow 0$.

6. Quantitative analysis of the linear sampling method. We have seen in the previous two sections that the norm of the regularized solutions as well as the magnitude of the regularization parameter strongly depend on the source representability (19) of the right-hand side g . In the context of the Linear Sampling Method this representability may be used to distinguish different points in the plane or the region of interest.

Accordingly we introduce the sets

$$(47) \quad \Omega_\nu = \{z \in \mathbb{R}^2 : g_z \in \mathcal{R}(|F|^\nu)\}, \quad 0 \leq \nu \leq 1,$$

where we denote by g_z the right-hand side (6) of the far field equation (5) corresponding to the sampling point $z \in \mathbb{R}^2$. We conclude from (17) that

$$(48) \quad \Omega_\nu \subset \Omega_\mu, \quad 0 \leq \mu < \nu \leq 1,$$

where the largest set Ω_0 coincides with \mathbb{R}^2 by virtue of (18), i.e., Ω_0 contains every sampling point. Moreover, because of the theoretical foundation of the Factorization Method (see [14]) there is a strong connection between these nested sets and our inverse scattering problem: namely, $\Omega_{1/2}$ coincides with the interior of the support of the true obstacles, i.e.,

$$(49) \quad \Omega_{1/2} = \Omega^\circ.$$

In the same spirit we subsequently denote by

$$(50) \quad \nu(z) = \sup \{ \nu > 0 : z \in \Omega_\nu \}$$

the so-called convergence abscissa of the exponent in the source condition for g_z of (6) associated with the sampling point $z \in \mathbb{R}^2$.

Ultimately, we argue that the contour lines of usual reconstructions of the Linear Sampling Method approximate, roughly speaking, boundaries of the nested sets Ω_ν , or level lines of the function $\nu = \nu(z)$. It then follows from (49) that one of these contour or level lines is close to the boundaries of the scattering obstacles, which is what is observed in practice.

To be more precise we recall, cf. Section 3 and the notation in there, that reconstructions of the Linear Sampling Method either consist of a plot of the norms of the regularized approximations $f^{\delta, \varepsilon}$ (Method I) or of the corresponding regularization parameters $\alpha_{\delta, \varepsilon}$ (Method II). In Method I the plot usually employs a logarithmic scale, whereas the initiators of Method II [8] refrained from using a logarithmic scale. Since $\delta = 0$ in the code from [8] this preference is reasonable in the light of

Example 1, cf. (46); when $\varepsilon = 0$, however, a logarithmic scale is more appropriate in Method II as well, compare (25) and Theorem 4.2.

In the following section we therefore show plots of the following four functions of z :

$$(51a) \quad \varphi_\delta(z) = \log \|f^{\delta,0}\| / |\log \delta|,$$

$$(51b) \quad \psi_\varepsilon(z) = \log \|f^{0,\varepsilon}\| / |\log \varepsilon|,$$

$$(51c) \quad \rho_\delta(z) = \log \alpha_{\delta,0} / \log \delta,$$

$$(51d) \quad \gamma_\varepsilon(z) = \alpha_{0,\varepsilon} / \varepsilon^2.$$

The functions φ_δ and ρ_δ correspond to the case $\varepsilon = 0$ of Section 4, whereas ψ_ε and γ_ε correspond to $\delta = 0$ as in Section 5. Note that neither the logarithms nor the divisors in (51) do affect the form of the contour lines. According to (24) we can now, for example, estimate

$$\varphi_\delta(z) \leq \frac{\log c}{|\log \delta|} + \frac{1 - \nu(z)}{\nu(z)},$$

provided that $\delta < 1$, and where the constant c is independent of δ , but still depends on ν and on z . We even know from Theorem 4.3 that the asymptotic upper bound $(1 - \nu(z))/\nu(z)$ is sharp as $\delta \rightarrow 0$. This indicates that

$$(52a) \quad \varphi_\delta(z) \lesssim (1 - \nu(z))/\nu(z)$$

for δ sufficiently small, although this approximation is no rigorous bound, as we have little to no control on the magnitude of the constant c in (24). Similarly, we expect

$$(52b) \quad \psi_\varepsilon(z) \lesssim 1 - \nu(z),$$

$$(52c) \quad \rho_\delta(z) \lesssim 2/\nu(z),$$

whenever δ and ε go to zero. According to (49) the particular level line corresponding to $\nu = 1/2$ of either of these three functions should provide a good guess of the boundaries of the true scattering obstacles.

7. Example: Scattering from the unit disk. To put our results in a realistic perspective we consider now in some detail the special situation when Ω is a disk of radius R centered at the origin, because for this example the singular value decomposition of the (exact) far field operator F and the corresponding expansion of the right-hand side $g = g_z$ of (6) are explicitly known, cf., e.g., [5].

To be specific, the singular functions of the associated far field operator are given by the trigonometric basis $\{e^{in\phi}\}_{n \in \mathbb{Z}}$, where ϕ denotes the polar angle of $\hat{x} \in S$, and

$$\lambda_n = \sqrt{\frac{2}{\pi k}} \left| \frac{J_n(kR)}{H_n^{(1)}(kR)} \right|, \quad n \in \mathbb{Z},$$

are the associated singular values. According to the Jacobi-Anger expansion, cf., e.g., [6], we can develop g_z for $z = r(\cos \theta, \sin \theta)$ into the trigonometric series

$$g_z(\cos \phi, \sin \phi) = \frac{e^{i\pi/4}}{\sqrt{8\pi k}} \sum_{n=-\infty}^{\infty} e^{-in(\theta+\pi/2)} J_n(kr) e^{in\phi}, \quad 0 \leq \phi < 2\pi,$$

and therefore, by Picard’s theorem, the set Ω_ν of (47) consists of all $z \in \mathbb{R}^2$ for which the infinite series

$$\sum_{n=0}^{\infty} \left| \frac{J_n^2(kr)}{J_n^{2\nu}(kR)} \right| |H_n^{(1)}(kR)|^{2\nu}, \quad r = \|z\|,$$

converges. Since $J_n(0) = 0$ for $n \neq 0$, and

$$\left| \frac{J_n^2(kr)}{J_n^{2\nu}(kR)} \right| |H_n^{(1)}(kR)|^{2\nu} \sim \frac{2^{2\nu-1}}{\pi} n^{-1} \left(\frac{ek}{2n}\right)^{2n(1-2\nu)} \left(\frac{r}{R^{2\nu}}\right)^{2n}$$

as $n \rightarrow \infty$ and $r \neq 0$, we conclude that

$$(53) \quad \Omega_\nu = \begin{cases} \{0\}, & 1/2 < \nu \leq 1, \\ \Omega^\circ, & \nu = 1/2, \\ \mathbb{R}^2, & 0 \leq \nu < 1/2. \end{cases}$$

This seems to indicate that the entire plane \mathbb{R}^2 is divided in only three separate regions that could be distinguished according to our approach. However, as always, computer results are considerably more subtle, as we shall illustrate for the case $R = 1$, i.e., for scattering from the unit disk. In the standard IEEE arithmetic with roughly 16 relevant decimal digits only 17 singular values of the far field operator corresponding to the unit disk Ω are above machine precision, and hence, the source condition (19) needs to be interpreted on a different level:

We say that $g \in \mathcal{L}^2(S)$ satisfies a *discrete source condition* with exponent $\tilde{\nu} > 0$, if

$$(54) \quad (I - E_{\text{eps}})g = (I - E_{\text{eps}})(FF^*)^{\tilde{\nu}/2}w \quad \text{for some } w \in \mathcal{L}^2(S) \text{ with } \|w\| = 1.$$

Here again, $\{E_\lambda\}$ is the spectral family of FF^* , and eps refers to the relevant absolute precision of the given computer approximation of FF^* . Note that even for $\text{eps} = 0$ the above definition differs from the classical one in (19) because of the constraint on w . We nevertheless incorporate this constraint because the asymptotic results from Sections 4 and 5 all somehow involve the norm of w and therefore deteriorate when $\|w\|$ gets either large or small.

An appealing consequence of (54) is that the discrete source condition defines a continuous function $\tilde{\nu}(z)$ which maps $z \in \mathbb{R}^2$ onto the unique positive number $\tilde{\nu}$ which satisfies (54) for $g = g_z$. This is in contrast to the function $\nu(z)$ of (50), which may have jump discontinuities, cf. (53). Note that for a disk centered at the origin the values of ν and $\tilde{\nu}$, as well as the four functions from (51) only depend on the norm $r = \|z\|$ of z , just as the Fourier coefficients of g_z do.

We claim that the expected bounds of (52) will rather depend on $\tilde{\nu}(z)$ than on $\nu(z)$. To substantiate this claim we provide computational results for $R = 1$ and $k = 1$: Figure 1 shows a plot of $\tilde{\nu}$ over the radius r of the sampling point z , together with the three approximations ν_φ , ν_ρ , and ν_ψ , that are obtained when the respective inequalities (52) are considered to be equalities and are solved for ν , i.e.,

$$(55) \quad \nu_\varphi(z) = \frac{1}{\varphi_\delta(z) + 1}, \quad \nu_\rho(z) = \frac{2}{\rho_\delta(z)}, \quad \nu_\psi(z) = 1 - \psi_\varepsilon(z).$$

The corresponding parameters have been set to be $\delta = 10^{-6}$ and $\varepsilon = 10^{-6}$, respectively. (See the following section concerning details about the numerical implementation.)

This plot is interesting in several respects. First, the function $\tilde{\nu}$ is, as expected, continuous and strictly decreasing; it is therefore well suited to distinguish different

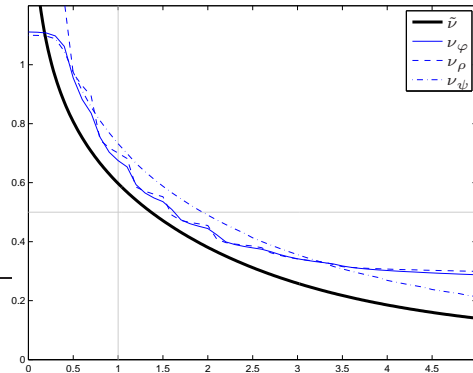


FIGURE 1. Approximations of ν for a scattering circle of radius $R = 1$

parts of our region of interest. Note, however, that $\tilde{\nu} > 1/2$ at $r = 1$, and therefore the calibration of the Linear Sampling Method, i.e., the selection of an appropriate contour line, will be a delicate issue in implementations of the method; we will briefly return to this problem in Section 8.

Second, the three graphs of ν_φ , ν_ρ , and ν_ψ are all qualitatively similar to the one of $\tilde{\nu}$. This may serve as a justification of our analysis of the Linear Sampling Method, although these approximations are not too close to $\tilde{\nu}$ quantitatively. Of course, this should not be a surprise because the identities (55) are severe oversimplifications of our theoretical results, as they (i) ignore the inequality signs in (52), and (ii) the fact, that the analysis in Sections 4 and 5 comes with quite a number of generic constants (which, in fact, all depend on z).

8. More numerical examples. While the previous section provides some limitations of our approach, we now present additional numerical results to illustrate potential benefits from our work. In all our numerical results the wave number has been set to be $k = 1$, and we use 128 incoming waves with equidistant directions $d \in S$ and corresponding measurements of the far field. These data are generated using a boundary element method.

To begin with we start with the famous kite-shaped obstacle from the pertinent literature. Figure 2 shows the reconstructions of the four variants of the Linear Sampling Method described in Section 6, i.e., color coded plots of the four functions φ_δ , ρ_δ , ψ_ϵ , and γ_ϵ of (51). These reconstructions use the same parameters $\delta = 10^{-6}$, resp. $\epsilon = 10^{-6}$, as in the previous section. Reconstructions with Method I are shown in the left hand column, the right hand column corresponds to Method II; the reconstructions using $\epsilon = 0$ are in the top row, those with $\delta = 0$ are in the bottom row. In these color coded plots the position of the kite phantom is emphasized by a bold solid black line, and the respective level lines corresponding to the ideal value $\nu = 1/2$ are indicated as white lines; in theory these level lines should coincide with the boundary of the scattering obstacle. In none of our reconstructions this happens to be the case, but except for the last plot there is always one level line which does agree very well with $\partial\Omega$. These white dashed level lines correspond to the numbers

$$(56) \quad \nu_\varphi = 0.67, \quad \nu_\rho = 0.68, \quad \text{and} \quad \nu_\psi = 0.75,$$

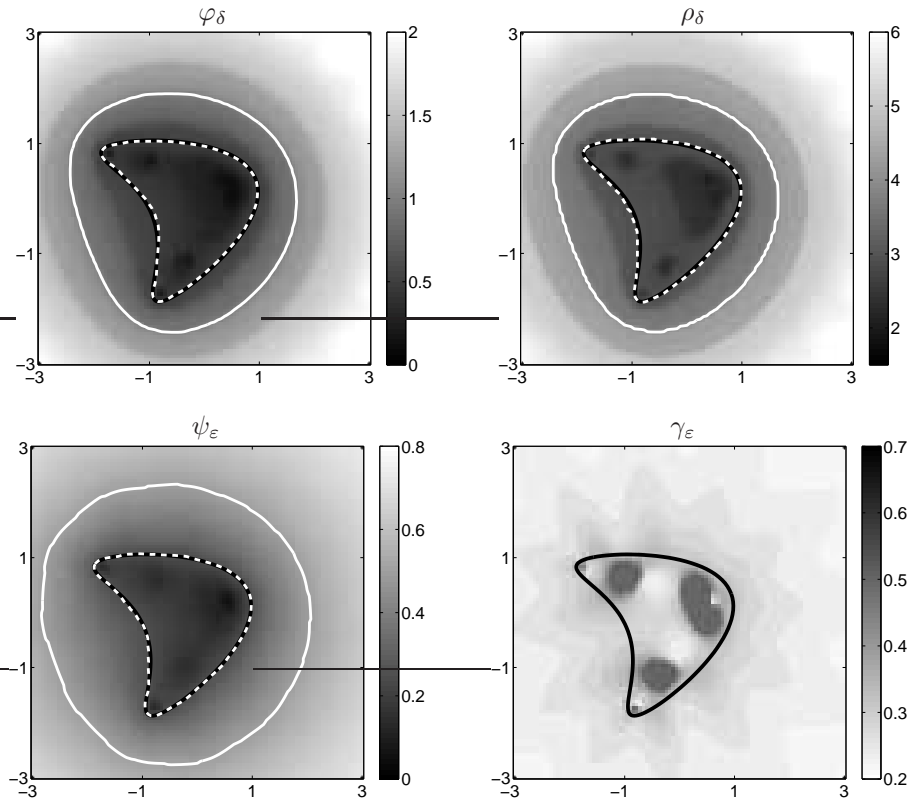


FIGURE 2. Reconstructions of a kite according to the four functions (51)

respectively. Note that these numbers match very well with the corresponding function values near the boundary of the scattering circle from the previous section, cf. Figure 1.

Besides, the first three plots in Figure 2 are also very similar to each other, although this depends on the respective color maps, of course. The plot of γ_ε , however, is clearly different: This plot only reveals some smaller features within the obstacle, and none of the level lines is a reasonable approximation of the kite's boundary. To a certain extent the smaller features can also be seen in the other plots; it is therefore possible that the total field u has an analytic continuation into the obstacle, right up to these smaller domains.

Figure 3 presents in the same way numerical results for two scattering objects, one kite and one ellipse, using the same parameters $\delta = 10^{-6}$ and $\varepsilon = 10^{-6}$ as before. This figure nicely underlines the well-known fact that the Linear Sampling Method is able to reconstruct multiple scatterers without the need to know their number in advance.

What is remarkable here is that the dashed reconstructions of the two obstacles correspond to the very same values of ν as before, cf. (56). (We remark, that the marginally larger value $\nu_\psi = 0.76$ would have given a slightly better reconstruction of the obstacles in the third plot.) For this example the plot of ψ_ε yields a better, namely smoother, reconstruction of the two obstacles, because the level lines of the two plots in the top row of Figure 3 exhibit oscillations that are not present in the

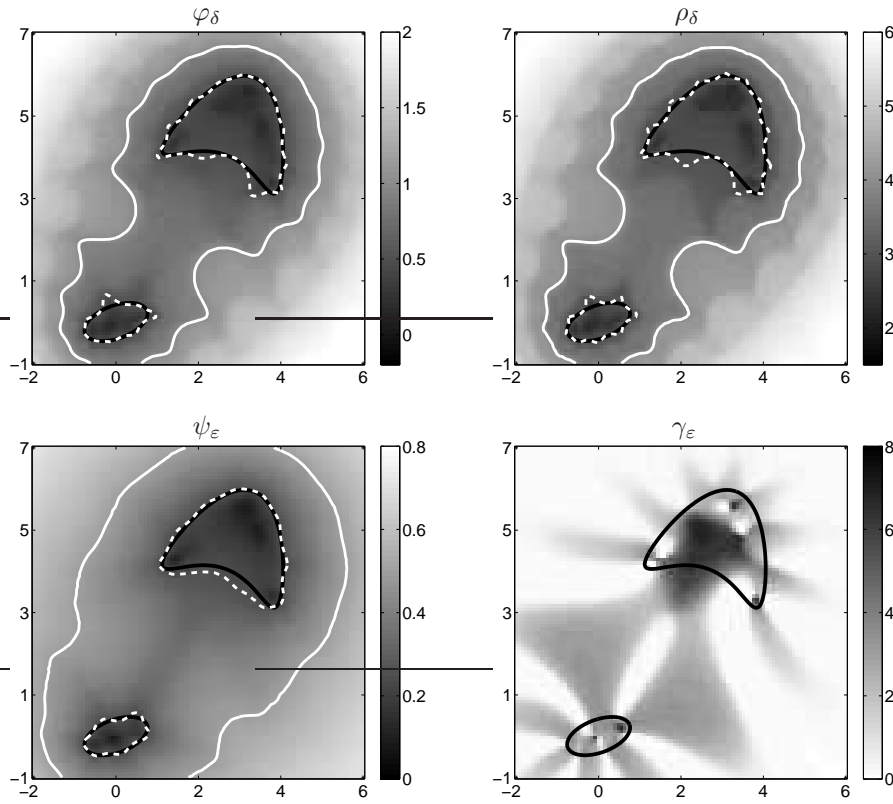


FIGURE 3. Reconstructions of two objects according to the four functions (51)

third plot. The plot of γ_ε is absolutely useless; it is significantly worse than in the previous example.

Finally, we reconsider the kite example, but this time we use noisy data. To be specific we use the same computed far field as above, but add a Gaussian random vector on top of these data such that

$$(57) \quad \|\tilde{F} - F\|_{\mathcal{L}^2(S) \rightarrow \mathcal{L}^2(S)} = \varepsilon := 10^{-2}.$$

To put this into perspective we note that in this example $\|F\|_{\mathcal{L}^2(S) \rightarrow \mathcal{L}^2(S)} \approx 0.72$, such that the amount of noise we use is slightly above 1 %.

As before, Figure 4 shows the corresponding four reconstructions, this time with parameters $\delta = 10^{-2}$ and $\varepsilon = 10^{-2}$ because of (57). In these plots the level lines corresponding to $\nu = 0.5$ are mostly outside the region of interest, but again, the first three plots have (white dashed) level lines which approximate the obstacle reasonably well. The corresponding values of ν , however, are significantly larger than in (56), namely

$$\nu_\varphi = 1.13, \quad \nu_\rho = 1.16, \quad \text{and} \quad \nu_\psi = 1.07.$$

In fact, it comes as no surprise (as the discrete source condition depends on the precision \mathbf{eps} of the relevant far field approximation) that the exponent $\tilde{\nu}$ of (54) increases as the number of eigenvalues above \mathbf{eps} decreases – and so do the appropriate approximations of $\tilde{\nu}$.

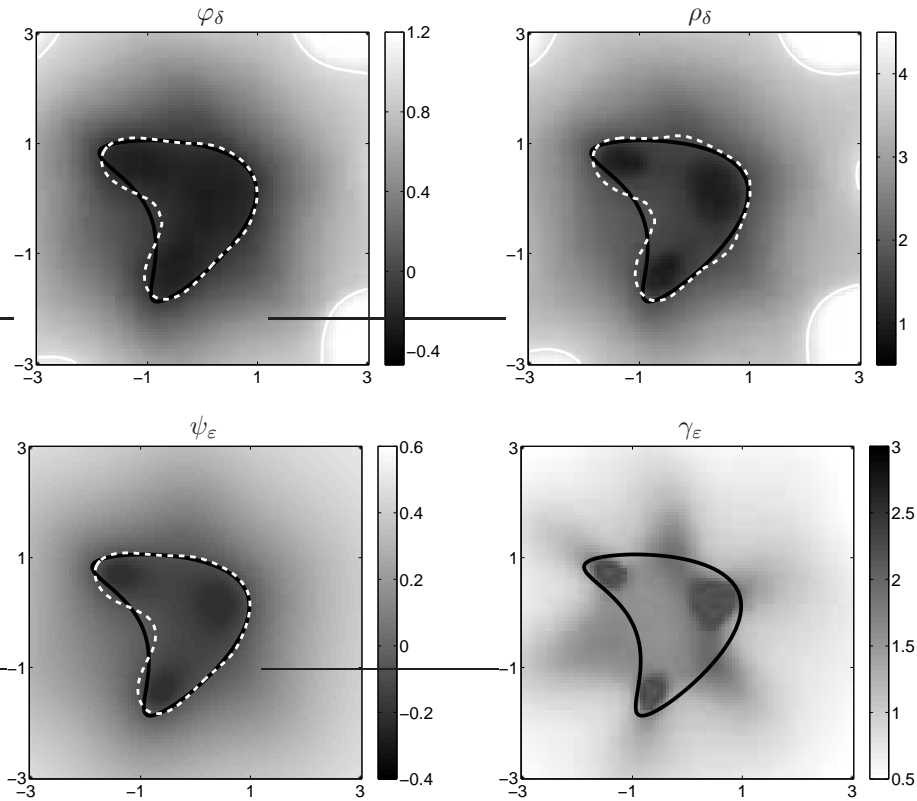


FIGURE 4. Reconstructions of the kite using noisy data

As in all previous examples, the level lines of γ_ε are very poor approximations of $\partial\Omega$.

9. Conclusions. Our theoretical and numerical results provide significant evidence that implementations of the Linear Sampling Method according to Method I (i.e., based on the norms of the Tikhonov approximations) provide good reconstructions of the scattering obstacles, at least when the Factorization Method is known to work. With the classical Morozov principle (11) reconstructions can also be based on the size of the regularization parameter (Method II). In either case the asymptotic analysis of these regularization methods opens up some possibility to calibrate the method, i.e., to predetermine values of appropriate level curves to reconstruct $\partial\Omega$. These levels appear to depend on the size of the parameters δ and ε on the one hand, and on the wave number and the diameter of the obstacles on the other hand, but only to a lesser extent on the specific form of the scatterers.

Our results do not support the use of Method II in combination with the modified discrepancy principle (34). In fact, taking also the numerical results from [8] into account we find that this approach can only be used to locate the approximate positions of the scatterer(s) but not really their shapes.

We finally remark that our analysis immediately extends to the Factorization Method, where instead of (5) one is interested in solutions of $Gf = g_z$ with g_z as before and $G = |F|^{1/2}$. As $\mathcal{R}(|F|^\nu) = \mathcal{R}(|G|^{2\nu})$, the level lines of the corresponding

functions $\nu(z)$, or $\tilde{\nu}(z)$, respectively, are the same as in our approach *in the exterior of Ω* , where $g_z \notin \mathcal{R}(G)$. In the interior of Ω , however, the functions φ_δ and ψ_ε of (51) will go to zero for the Factorization Method as δ and ε go to zero, and this is the reason why – on the grounds of Method I – the shapes of the scatters are better to detect visually with the Factorization Method than with the Linear Sampling Method.

Acknowledgements. The author is pleased to thank Andreas Kirsch for providing his codes to generate far field data for the numerical examples.

REFERENCES

- [1] T. Arens, *Why linear sampling works*, Inverse Problems, **20** (2004), 163–173.
- [2] T. Arens and A. Lechleiter, “The Linear Sampling Method Revisited,” manuscript, 2007.
- [3] F. Cakoni and D. Colton, “Qualitative Methods in Inverse Scattering Theory: An Introduction,” Interaction of Mechanics and Mathematics, Springer-Verlag, Berlin, 2006.
- [4] A. Charalambopoulos, D. Gintides and K. Kiriaki, *The linear sampling method for the transmission problem in three-dimensional linear elasticity*, Inverse Problems, **18** (2002), 547–558.
- [5] D. Colton and A. Kirsch, *A simple method for solving inverse scattering problems in the resonance region*, Inverse Problems, **12** (1996), 383–393.
- [6] D. Colton and R. Kress, “Inverse Acoustic and Electromagnetic Scattering Theory,” 2nd Ed., Applied Mathematical Sciences, 93, Springer, Berlin, 1998.
- [7] D. Colton and P. Monk, *A linear sampling method for the detection of leukemia using microwaves II*, SIAM J. Appl. Math., **60** (1999), 241–255.
- [8] D. Colton, M. Piani and R. Potthast, *A simple method using Morozov’s discrepancy principle for solving inverse scattering problems*, Inverse Problems, **13** (1997), 1477–1493.
- [9] H. W. Engl, M. Hanke and A. Neubauer, “Regularization of Inverse Problems,” Mathematics and its Applications, **375**, Kluwer Academic Publishers Group, Dordrecht, 1996.
- [10] B. Gebauer, M. Hanke, A. Kirsch, W. Muniz and C. Schneider, *A sampling method for detecting buried objects using electromagnetic scattering*, Inverse Problems, **21** (2005), 2035–2050.
- [11] I. S. Gradshteyn and I. M. Ryzhik, “Table of Integrals, Series and Products,” 7th Ed., Academic Press, New York, 2007.
- [12] C. W. Groetsch, “The Theory of Tikhonov Regularization for Fredholm Integral Equations of the First Kind,” Research Notes in Mathematics, **105**, Pitman (Advanced Publishing Program), Boston, MA, 1984.
- [13] H. Haddar and P. Monk, *The linear sampling method for solving the electromagnetic inverse medium problem*, Inverse Problems, **18** (2002), 891–906.
- [14] A. Kirsch, *Characterization of the shape of a scattering obstacle using the spectral data of the far field operator*, Inverse Problems, **14** (1998), 1489–1512.
- [15] A. Kirsch and N. Grinberg, “The Factorization Method for Inverse Problems,” Oxford University Press, Oxford, 2008.
- [16] P. Monk, “Finite Element Methods for Maxwell’s Equations,” Numerical Mathematics and Scientific Computation. Oxford University Press, New York, 2003.
- [17] V. A. Morozov, *On the solution of functional equations by the method of regularization*, Dokl. Akad. Nauk SSSR, 167, 510–512 (Russian), translated as Soviet Math. Dokl., **7** (1966), 414–417.
- [18] V. A. Morozov, “Methods for Solving Incorrectly Posed Problems,” Translated from the Russian by A. B. Aries. Translation edited by Z. Nashed. Springer-Verlag, New York, 1984.
- [19] S. Nintcheu Fata and B. B. Guzina, *A linear sampling method for near-field inverse problems in elastodynamics*, Inverse Problems, **20** (2004), 713–736.

- [20] A. Tacchino, J. Coyle and M. Piana, *Numerical validation of the linear sampling method*, Inverse Problems, **18** (2002), 511–527.
- [21] G. M. Vainikko, *The discrepancy principle for a class of regularization methods*, USSR Comp. Math. Math. Phys., **22** (1982), 1–19.
- [22] G. M. Vainikko, *The critical level of discrepancy in regularization methods*, USSR Comp. Math. Math. Phys., **23** (1983), 1–19.

Received June 2008; revised June 2008.

E-mail address: hanke@math.uni-mainz.de